

EvoGP: A GPU-accelerated Framework for Tree-based Genetic Programming

Lishuang Wang, Zhihong Wu, Kebin Sun, Zhuozhao Li, and Ran Cheng, *Senior Member, IEEE*

Abstract—Tree-based Genetic Programming (TGP) is a key evolutionary algorithm widely used in symbolic regression, feature engineering, and scientific modeling. Its high computational demands make GPU acceleration essential for scalable and high-performance evolutionary computation. However, GPU acceleration of TGP faces three key challenges: inefficient tree encoding, highly heterogeneous genetic operations, and limited parallelism in fitness evaluation. To address these challenges, we introduce EvoGP, a comprehensive GPU-accelerated TGP framework. First, we design a tensorized encoding scheme to represent tree with different structures as tensors with the same shape, optimizing memory access and enabling efficient parallel execution. Second, we propose a unified parallel framework for genetic operations by leveraging shared computational primitives and implementing dedicated CUDA kernels for scalable performance. Third, we present a fully parallel fitness evaluation strategy for symbolic regression, exploiting both population-level and data-level parallelism to maximize GPU utilization. Moreover, we implement a comprehensive library to provide rich algorithm operators and benchmark problems. EvoGP is extensively tested on various tasks, including symbolic regression, classification, and robotics control, demonstrating its versatility and effectiveness across diverse application scenarios. Experimental results show that EvoGP achieves up to a 140.89 \times speedup over the state-of-the-art GPU-based TGP implementation, while maintaining or exceeding the accuracy of baseline methods. EvoGP is open-source and accessible at: <https://github.com/EMI-Group/evogp>.

Index Terms—Genetic programming, parallel algorithm, graphic processing unit (GPU), compute unified device architecture (CUDA).

I. INTRODUCTION

GENETIC Programming (GP) [1] is an evolutionary algorithm that autonomously evolves programs by emulating the principles of natural selection and genetic inheritance. Unlike black-box models such as neural networks, GP provides human-readable solutions, making it a highly interpretable machine learning paradigm [2]. Depending on the representation of programs, GP is categorized into several variants, including Linear GP (LGP) [3], [4], Cartesian GP (CGP) [5], [6], Gene Expression Programming (GEP) [7], and Grammatical Evolution (GE) [8]. Among these, TGP is the most widely adopted approach [9], [10]. TGP represents programs as hierarchical tree structures, where nodes correspond

The first three authors contributed equally to this work.

Lishuang Wang, Zhihong Wu, Kebin Sun, and Zhuozhao Li are with the Department of Computer Science and Engineering, Southern University of Science and Technology, Shenzhen 518055, China. E-mails: {wanglishuang22, zhihong2718, sunkebin.cn}@gmail.com, lizz@sustech.edu.cn.

Ran Cheng is with the Department of Data Science and Artificial Intelligence, and Department of Computing, The Hong Kong Polytechnic University, Hong Kong SAR, China. E-mail: ranchengcn@gmail.com. (*Corresponding author: Ran Cheng*).

to functions or operations, and edges denote data flow. This structured representation allows flexible program evolution through genetic operations such as crossover, mutation, and selection. As a result, TGP has been successfully applied to a wide range of tasks, including regression [11]–[14], classification [15], [16], feature learning [17], [18], image and signal processing [19], production scheduling [20], etc.

TGP evolves a population of candidate solutions through iterative genetic operations such as selection, crossover and mutation, followed by fitness evaluation. However, this process is computationally intensive, especially for large populations, as each generation requires performing genetic operations and evaluating every individual. Like other evolutionary algorithms, TGP is inherently parallelizable, since these operations can be executed independently across individuals. Consequently, leveraging modern hardware architectures, particularly GPUs, has become a compelling approach to alleviating computational overhead. In recent years, GPU acceleration has gained widespread adoption in evolutionary computation, with studies demonstrating significant speedups across various evolutionary algorithms [21]–[26]. Given these advancements, developing efficient GPU-accelerated techniques for TGP is crucial to enhancing its scalability and performance.

Despite the potential of GPU acceleration in TGP algorithms, designing an efficient TGP implementation for GPUs presents three major challenges. First, existing tree-encoding methods are not directly suitable for GPU execution. The two primary encoding strategies, pointer-based tree encoding [27], [28] and prefix encoding [29]–[31], both exhibit significant inefficiencies when applied to GPUs. Pointer-based tree encoding suffers from frequent global memory accesses and noncontiguous memory storage, leading to poor memory coalescing and increased latency. Prefix encoding, while compact, loses structural information, requiring costly tree-parsing operations that introduce excessive logical branching on GPUs. Additionally, both encoding methods struggle to handle dynamic tree growth efficiently, necessitating memory reallocation, which further degrades GPU performance [32].

Second, the diverse variants of genetic operations in TGP, such as crossover and mutation, pose significant challenges for GPU acceleration. Each variant modifies the tree differently, making a comprehensive GPU implementation a substantial engineering effort. Additionally, some complex genetic operations require tree parsing and reconstruction, which are difficult to parallelize efficiently on GPUs.

Third, symbolic regression is one of the most important applications of TGP. However, the current state-of-the-art symbolic regression [31] fitness evaluation primarily relies

on data-parallelism, which enables simultaneous processing of different data points but does not support evaluating multiple trees in parallel. This limitation becomes particularly problematic when the number of data points in the symbolic regression task is limited. In such cases, GPU computational resources are underutilized, leading to inefficiencies in execution.

Currently, several existing TGP libraries provide hardware acceleration. DEAP [29] and gplearn [30] enable parallel fitness evaluation on CPUs through multiprocessing, leveraging multi-core architectures to speed up computations. KarrroGP [27] and TensorGP [28] employ TensorFlow-based vectorization to evaluate GP trees on multiple data points simultaneously, improving the inference speed through GPU-accelerated computation. SR-GPU [31], the current state-of-the-art TGP implementation, further advances GPU-based evaluation by implementing CUDA kernels specifically designed for symbolic regression. These implementations focus solely on accelerating the evaluation phase, leaving other essential TGP operations such as crossover and mutation unoptimized. Moreover, during the evaluation process, they do not support parallel evaluation of multiple individuals from the population on the GPU, which limits scalability in large-scale evolutionary experiments.

To overcome these challenges, we introduce EvoGP, the first comprehensive GPU-accelerated TGP framework. Firstly, we extend prefix encoding by introducing a maximum-length constraint, ensuring that all trees in the population share a uniform tensor shape. This design eliminates memory reallocation overhead and enables efficient, fully parallel tree operations on the GPU. Then, we systematically analyze all mutation and crossover operations in TGP and extract their core computational primitives. By identifying these shared components, we develop a unified GPU-accelerated framework that efficiently supports various mutation and crossover variants, significantly improving computational efficiency. Finally, we propose a novel fitness evaluation strategy for symbolic regression that leverages both population-level and data-point-level parallelism. This hybrid parallelism ensures that GPU resources are fully utilized, leading to substantial performance improvements. Experimental results demonstrate that EvoGP achieves up to a 140.89 \times speedup over the state-of-the-art GPU-based TGP implementation [31].

The rest of this paper is organized as follows. Section II introduces the fundamentals of TGP, outlines the GPU computing model, and discusses existing TGP implementations. Section III presents the main challenges associated with GPU acceleration of TGP. In Section IV, we describe our proposed approach to address these challenges. Section V details the implementation of the EvoGP framework. In Section VI, we verify the effectiveness of our approach through experimental evaluation. Finally, a conclusion is drawn in the last section.

II. BACKGROUND AND RELATED WORKS

In this section, we briefly review the TGP algorithm and introduce the GPU architecture and CUDA. Finally, we introduce the existing TGP implementations.

A. Tree-based Genetic Programming

TGP is a core evolutionary algorithm widely used in symbolic regression [11]–[14], feature engineering [15], [17], [18], complex system design [33]–[36], and robotic control [37]–[39]. In TGP, solutions are represented as trees, which define the flow of computation from inputs to output. Formally, a TGP tree can be described as

$$T = (V, E, r),$$

where V is the set of nodes, $E \subseteq V \times V$ is the set of edges, and $r \in V$ is the distinguished root node. Every node $v \in V \setminus \{r\}$ has exactly one parent.

A TGP tree represents a function Func that maps an input vector \mathbf{x} to an output y :

$$y = \text{Func}(\mathbf{x}).$$

The computation proceeds in a bottom-up manner: each node v calculates its result $\text{res}[v]$, and the root node's result $\text{res}[r]$ serves as the final output y .

Each node in the tree is represented by a tuple $v = (t, \text{val})$, where t is the node type, and val stores the node's value. Nodes in a TGP tree fall into three categories:

Constant Node: Represents a numerical constant. Its computation is:

$$\text{res}[v] = \text{val}.$$

Variable Node: Represents an input variable. Here, val indicates the index of the input vector \mathbf{x} , and its computation is:

$$\text{res}[v] = \mathbf{x}[\text{val}].$$

Function Node: Represents a mathematical or logical function. In this case, val specifies the function type f , and its computation is:

$$\text{res}[v] = f(\text{res}[c_1], \text{res}[c_2], \dots, \text{res}[c_n]),$$

where c_1, c_2, \dots, c_n are the children of the node.

By using this tree-based representation, TGP supports flexible modeling of mathematical expressions and decision processes, which constitute the foundation of Genetic Programming. Fig. 1 shows an example of TGP trees.

TGP iteratively refines a population of trees through a series of genetic operations, including selection, crossover, and mutation, to evolve optimal or near-optimal solutions. Selection is a process that chooses individuals from the population based on their performance, ensuring that better-performing solutions have a higher probability of propagating to subsequent generations. Crossover involves exchanging information between selected parent trees, facilitating genetic diversity and exploration of the solution space. Mutation introduces random modifications by altering nodes or branches within an individual tree, thus promoting further diversity and preventing premature convergence. [40] The evolutionary process is described in Algorithm 1.

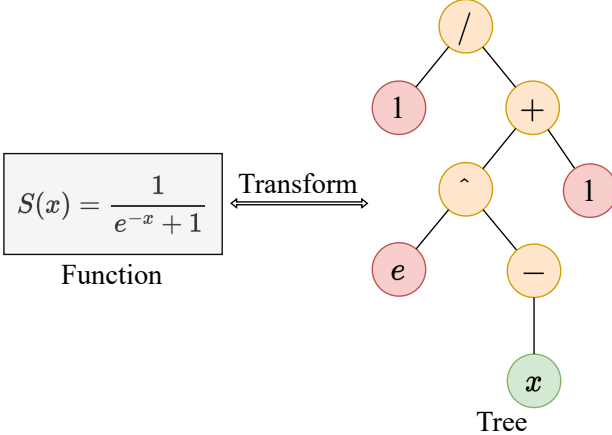


Fig. 1: An example of a tree. In TGP, a computational process is represented as a tree structure. The tree shown in the figure illustrates the sigmoid function. In the figure, the orange nodes represent function nodes, the red nodes represent constant nodes, and the green nodes represent variable nodes.

B. GPU Architecture and CUDA Programming

With the increasing demand for parallel computing, GPUs have evolved into highly efficient accelerators for data-intensive tasks. Modern GPUs consist of thousands of processing cores organized into Streaming Multiprocessors (SMs), enabling massive parallelism. The memory hierarchy includes high-latency global memory, multilevel caches (L1, L2) for faster access, and constant memory optimized for read-only data [41]. Since GPUs do not support dynamic memory management as CPUs, handling variable-sized data structures such as trees is challenging [42].

CUDA (Compute Unified Device Architecture) is a parallel computing platform and programming model developed by NVIDIA, designed to harness the computing power of GPUs for general purpose computing [43], [44]. One of the fundamental execution models in CUDA is SIMD (Single

Algorithm 1 Main Process of TGP

Require: Population size N ; Target fitness f_{target} ; Max generations count G ;
 $P \leftarrow$ Randomly generate N trees;
for $g = 1$ to G **do**
 $Fit \leftarrow$ Evaluate fitness values of P ;
 if $\max(Fit) \geq f_{\text{target}}$ **then**
 break
 end if
 $C \leftarrow$ The empty population.
 while Not enough trees in C **do**
 $Parent1, Parent2 \leftarrow$ Select parents;
 $Child \leftarrow \text{Crossover}(Parent1, Parent2)$;
 $Child \leftarrow \text{Mutation}(Child)$;
 $C \leftarrow C \cup \{Child\}$
 end while
end for
return $P[\arg \max(Fit)]$

Instruction, Multiple Threads) [45]. CUDA organizes parallel execution in a hierarchical manner, consisting of three key levels: grid, block, and thread. A CUDA kernel launches a grid of thread blocks, where each block contains multiple threads. These threads execute in parallel, and the execution is coordinated through shared memory, synchronization mechanisms, and optimizations of the memory hierarchy [32], [46].

C. Existing TGP Implementations

DEAP [29] is a general purpose evolutionary computation framework designed for flexibility and extensibility. It supports a wide range of evolutionary algorithms, including genetic programming, with features such as custom operators, comprehensive logging, and parallelization via multiprocessing.

gplearn [30], built on top of scikit-learn, provides tools for symbolic regression, classification, and transformation tasks. It offers customizable function sets, mutation, and crossover operators, making it suitable for feature engineering and interpretable machine learning. gplearn leverages joblib for parallel computation, enabling efficient evaluation of large populations.

KarooGP [27] is a genetic programming framework that integrates with TensorFlow [47], using its graph execution model to execute GP expressions as directed acyclic graphs (DAG). It is particularly useful for symbolic regression and classification tasks. KarooGP is designed to be user-friendly, providing a command-line interface for configuration and execution.

TensorGP [28] is a genetic programming engine built on TensorFlow's eager execution model. It simplifies the implementation of genetic programming tasks, particularly symbolic regression, by eliminating the need for DAG construction. TensorGP is designed with scalability in mind, leveraging TensorFlow's ecosystem to support high-performance computation.

SRGPU [31] focuses on symbolic regression tasks using CUDA for efficient parallel computation. Its core design maps GPU threads to process data points within the same individual, optimizing regression workflows. SRGPU is particularly designed for tasks that require large-scale data analysis, combining evolutionary computation with hardware acceleration.

III. CHALLENGES OF GPU ACCELERATION FOR TGP

In this section, we discuss three key challenges that hinder efficient GPU acceleration of TGP.

A. Inefficient Tree Encoding

TGP primarily employs two encoding schemes: pointer-based tree encoding [27], [28] and prefix encoding [29]–[31].

Pointer-based tree encoding represents trees as object structures in programming models, where each node stores pointers to its child nodes. This approach efficiently preserves the hierarchical relationships of the tree structure, enabling genetic operations such as subtree crossover by merely updating pointer references. However, the non-contiguous memory layout of tree nodes poses significant challenges for GPU acceleration. Additionally, frequent pointer dereferencing leads to excessive

non-coalesced global memory accesses, severely degrading computational performance.

Prefix encoding represents a tree using its prefix sequence, leveraging the fixed arity of nodes in TGP to fully encapsulate the tree structure without requiring explicit pointer-based connections. This encoding scheme offers a straightforward storage format with a contiguous memory layout, leading to improved memory access efficiency. However, its primary drawback lies in the lack of explicit structural information. During genetic operations, it is often necessary to parse the prefix sequence to determine subtree boundaries and sizes. This process involves extensive logical branching, which significantly hampers execution speed on GPUs.

Additionally, both encoding methods struggle with dynamic tree growth, as it requires frequent GPU memory reallocation, incurring high overhead and disrupting memory coalescing, which degrades performance.

B. Highly Heterogeneous Genetic Operations

The diverse genetic operations in TGP introduce significant challenges for GPU acceleration due to their structural complexity and variability. For instance, crossover operations can be categorized into leaf-biased crossover and normal crossover, while mutation includes multiple variants such as subtree mutation, hoist mutation, and insert mutation. Each of these variants modifies the tree structure differently, requiring distinct processing strategies.

Furthermore, new genetic operations are often introduced to optimize performance for specific tasks, further increasing the complexity of a comprehensive GPU implementation. Achieving efficient parallelization for such a diverse set of operations is a substantial engineering effort, as it involves handling dynamic tree modifications while maintaining memory coherence and minimizing thread divergence. Additionally, ensuring scalability in GPU acceleration remains a key challenge, as future extensions may require flexible and adaptive implementations that can efficiently incorporate novel genetic operations without significant overhead.

C. Limited Parallelism in Fitness Evaluation

Symbolic regression (SR) [11]–[14] is one of the primary applications of TGP, where the goal is to evolve mathematical expressions that best fit a given dataset. The fitness evaluation in SR typically measures how well a candidate expression approximates the target function by computing the loss over all given data points.

The state-of-the-art SR fitness evaluation method [31] predominantly rely on data-parallelism, where the loss for different data points is computed in parallel for a single tree. This approach leverages parallel reduction techniques to aggregate the individual losses into a single fitness value. However, to evaluate the entire population, the kernel must be launched iteratively for each tree, which introduces additional overhead.

While this data-parallel approach efficiently utilizes GPU resources when the number of data points is sufficiently large, it allows a single tree's computation to fully occupy available threads. However, it becomes inefficient when the dataset is

small. In such cases, individual tree evaluations fail to saturate the GPU, and the lack of population-level parallelism leads to significant underutilization of computational resources, resulting in execution inefficiencies.

IV. PROPOSED METHOD

In this section, we present our proposed method to address the challenges introduced in Section III.

A. Tensorized Encoding

To overcome the inefficiencies associated with both pointer-based and prefix encodings discussed in Section III-A, we propose a tensorized encoding scheme that addresses two major issues in TGP. First, it mitigates the need for repeated structural parsing of trees on GPUs, which introduces abundant logical branching and degrades performance. Second, it avoids frequent memory reallocation caused by dynamic tree growth, a well-known challenge for GPU-based systems.

We adopt prefix encoding, which stores the nodes of a tree in a contiguous sequence. Generally, a simple prefix sequence does not suffice to fully represent an arbitrary tree structure, as the number of children for each node may vary. However, in TGP, the number of children is determined by the node's type (t) and its value (val). For instance, *Constant* and *Variable* nodes have no children, whereas a *Function* node (e.g., sum) has two children. Consequently, for TGP applications, a single prefix sequence can encode all critical information about a tree's topology and values.

In existing implementations [31], prefix encoding typically consists of two arrays:

$$n_{\text{type}} = [t_1, t_2, \dots, t_n] \in \mathbb{R}^{\text{len}(T)},$$

$$n_{\text{val}} = [val_1, val_2, \dots, val_n] \in \mathbb{R}^{\text{len}(T)},$$

where t_i and val_i represent the type and value of the i -th node, respectively, and $\text{len}(T)$ denotes the total number of nodes in the tree T . Although this representation is compact, it does not store explicit structural information. As a result, operations such as subtree crossover or mutation typically require repeated parsing of the prefix sequence to locate subtrees, making GPU-based execution inefficient.

To remedy this, we introduce an additional array that records the size of each subtree:

$$n_{\text{size}} = [\text{size}(1), \text{size}(2), \dots, \text{size}(n)] \in \mathbb{R}^{\text{len}(T)},$$

where $\text{size}(i)$ indicates the size of the subtree rooted at the i -th node. By incorporating this subtree size array, one can directly determine the boundaries of any subtree in T , thereby obviating the need for costly tree parsing during genetic operations on the GPU.

Although prefix encoding provides a suitable representation for trees in TGP, it remains challenging to efficiently batch-process these structures on GPUs due to their variable sizes. To address this, we introduce a hyperparameter $|T|_{\text{max}}$, which denotes the maximum allowed number of nodes in a tree. Each

of the arrays n_{type} , n_{val} , and n_{size} is then padded with NaN values to form fixed-length arrays:

$$\begin{aligned}\hat{n}_{\text{type}} &= [t_1, t_2, \dots, \text{NaN}, \dots] \in \mathbb{R}^{|T|_{\max}}, \\ \hat{n}_{\text{val}} &= [val_1, val_2, \dots, \text{NaN}, \dots] \in \mathbb{R}^{|T|_{\max}}, \\ \hat{n}_{\text{size}} &= [\text{size}(1), \text{size}(2), \dots, \text{NaN}, \dots] \in \mathbb{R}^{|T|_{\max}}.\end{aligned}$$

Here, the actual tree data occupy the first $\text{len}(T)$ positions, and the remaining entries are filled with NaN. This padding strategy ensures that all trees share a consistent tensor shape, enabling straightforward GPU-friendly batching.

Once each tree is converted to padded arrays \hat{n}_{type} , \hat{n}_{val} , and \hat{n}_{size} , we concatenate them across the population dimension. Let P be the total number of trees in the population. Then, the population can be represented using three tensors:

$$\begin{aligned}P_{\text{type}} &= [\hat{n}_{\text{type}}^1, \hat{n}_{\text{type}}^2, \dots] \in \mathbb{R}^{P \times |T|_{\max}}, \\ P_{\text{val}} &= [\hat{n}_{\text{val}}^1, \hat{n}_{\text{val}}^2, \dots] \in \mathbb{R}^{P \times |T|_{\max}}, \\ P_{\text{size}} &= [\hat{n}_{\text{size}}^1, \hat{n}_{\text{size}}^2, \dots] \in \mathbb{R}^{P \times |T|_{\max}},\end{aligned}$$

where \hat{n}_{type}^i , \hat{n}_{val}^i , and \hat{n}_{size}^i are the padded arrays corresponding to the i -th tree. By unifying all trees into these fixed-shape tensors, genetic operators and fitness evaluations can be designed to leverage GPU parallelism effectively.

Fig. 2 provides a graphical overview of this tensorized encoding scheme. In summary, storing the subtree size array alongside prefix-encoded values enables rapid access to individual subtrees, while padding to a fixed length circumvents the overhead of dynamic memory allocation and irregular indexing on GPUs. As a result, this approach paves the way for an efficient and scalable implementation of TGP that fully exploits modern GPU architectures.

B. Unified Genetic Operation Framework

In order to address the challenges discussed in Section III-B regarding highly heterogeneous genetic operations, we propose a Unified Genetic Operation Framework for GPU-based TGP. Our key idea is to identify and accelerate the core *subtree exchange* procedure that underlies most TGP genetic operations, such as one-point crossover, subtree mutation, and hoist mutation. By offloading subtree exchange to the GPU, we enable a comprehensive and extensible set of genetic operations to be efficiently executed in parallel.

Subtree exchange refers to replacing a designated subtree of one tree with a subtree from another source. In conventional prefix encoding, this process can be computationally expensive because it involves tree parsing to determine subtree boundaries. However, our tensorized encoding obviates the need for extensive parsing by explicitly storing each node's subtree size. Consequently, subtree boundaries can be located through direct indexing, substantially reducing the complexity of subtree exchange.

We define the subtree exchange operation as

$$\text{exchange}(T_{\text{old}}, n, T_{\text{new}}) \rightarrow T^*,$$

where T_{old} is the original tree for subtree exchange, n denotes the root of the target subtree in T_{old} , and T_{new} is the subtree that will replace the original subtree rooted at n . Under

our tensorized encoding, each tree is represented by three tensors: \mathbf{n}_{type} , $\mathbf{n}_{\text{value}}$, and \mathbf{n}_{size} . We use \oplus to denote the tensor concatenation operation, and define

$$\begin{aligned}n_{\text{type}}^* &= n_{\text{type}}^{\text{old}}[1, 2, \dots, s] \oplus n_{\text{type}}^{\text{new}} \oplus n_{\text{type}}^{\text{old}}[e, e+1, \dots], \\ n_{\text{value}}^* &= n_{\text{value}}^{\text{old}}[1, 2, \dots, s] \oplus n_{\text{value}}^{\text{new}} \oplus n_{\text{value}}^{\text{old}}[e, e+1, \dots], \\ n_{\text{size}}^* &= n_{\text{size}}^{\text{updated}}[1, 2, \dots, s] \oplus n_{\text{size}}^{\text{new}} \oplus n_{\text{size}}^{\text{old}}[e, e+1, \dots],\end{aligned}$$

where $s = \text{index}(n)$ is the starting position of the subtree, and $e = s + n_{\text{size}}^{\text{old}}(n)$ is the ending position in T_{old} . The tensor $n_{\text{size}}^{\text{updated}}$ is computed by adding $n_{\text{size}}^{\text{new}}[0]$ to the subtree sizes of all ancestor nodes of n :

$$n_{\text{size}}^{\text{updated}}[i] = \begin{cases} n_{\text{size}}^{\text{old}}[i] + n_{\text{size}}^{\text{new}}[0], & \text{if } i \text{ is an ancestor of } n, \\ n_{\text{size}}^{\text{old}}[i], & \text{otherwise.} \end{cases}$$

By focusing on subtree exchange, we can efficiently implement virtually all TGP genetic operations. For instance, the one-point crossover, a fundamental crossover variant, replaces a random subtree of one parent with a random subtree from the other parent:

$$T^* = \text{exchange}(T_1, n, T_2^{\text{sub}}),$$

where T_1 and T_2 are parent trees, n is a random node in T_1 , and T_2^{sub} is a randomly selected subtree from T_2 .

Similarly, subtree mutation replaces a randomly selected subtree with a newly generated subtree:

$$T^* = \text{exchange}(T, n, T_{\text{new}}),$$

where T is the tree to be mutated, n is a random node in T , and T_{new} denotes the newly generated subtree. Fig. 3 provides a graphical overview of these genetic operations and their corresponding tensor transformation.

Once the subtree exchange operation is offloaded to the GPU, any genetic operator that can be decomposed into subtree exchange steps can be accelerated with minimal effort. Moreover, researchers can easily incorporate novel genetic operators into the framework by defining the required subtree selection or replacement strategies. As a result, this Unified Genetic Operation Framework greatly simplifies and unifies the process of designing GPU-accelerated TGP algorithms, facilitating both performance and extensibility.

C. Hybrid Parallelism in SR Evaluation

As mentioned in Section III-C, existing GPU-based symbolic regression (SR) evaluation methods [31] predominantly rely on data-level parallelism. In these methods, a single kernel invocation computes the fitness of one tree by evaluating it across all data points. This approach efficiently utilizes GPU resources when the dataset size is large, since each tree evaluation can occupy a substantial portion of the GPU's threads. However, it also requires launching a separate kernel for each individual in the population. When the population size grows, these repeated kernel launches introduce significant overhead, which limits overall efficiency.

To overcome this limitation, EvoGP employs a hybrid parallelism approach that distributes computation across both the population and data dimensions in a single kernel launch.

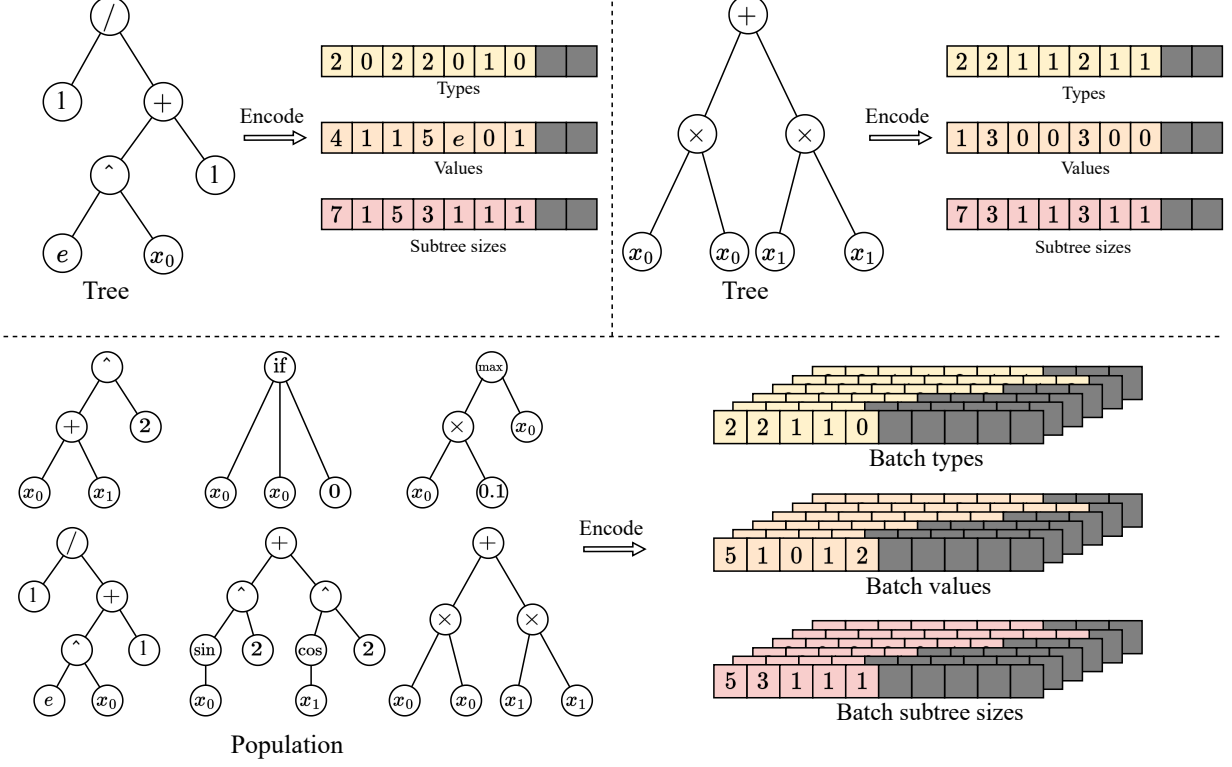


Fig. 2: Illustration of the tree encoding process. In tensorized encoding, a tree is encoded into three tensors: types, values, and subtree sizes. We use NaN padding to ensure that these tensors reach a uniform maximum size, allowing trees of different structures to be encoded into tensors of the same shape. This enables the encoding of an entire population of trees into three batched tensors.

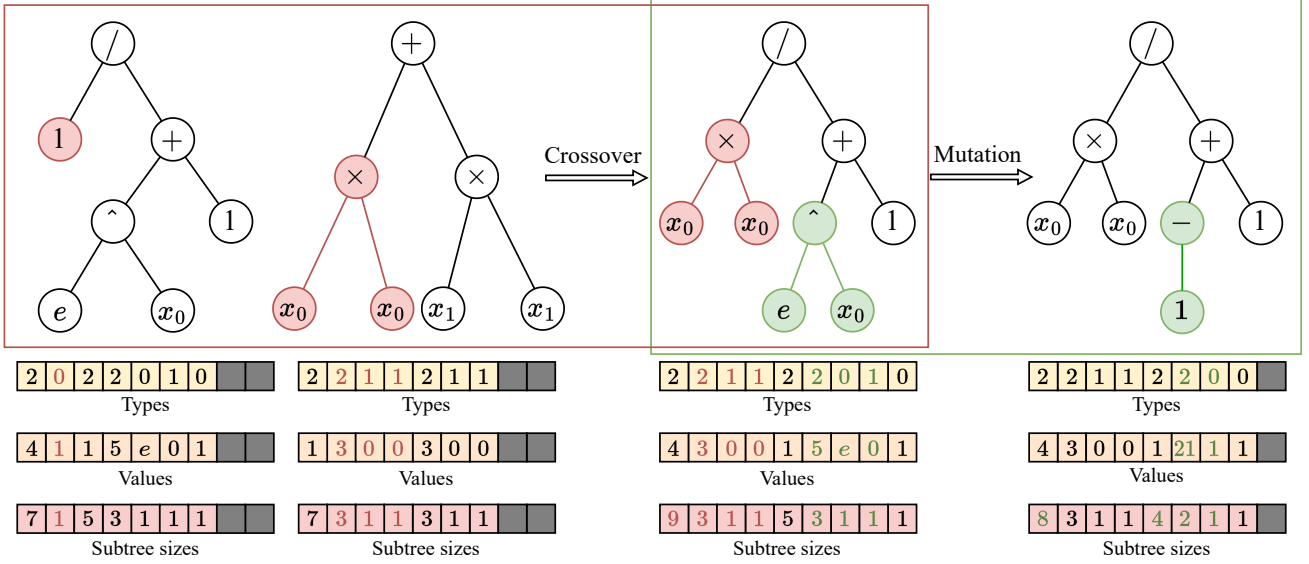


Fig. 3: An illustration of genetic operations in TGP. The upper part depicts the structural modifications of trees. The red box highlights the crossover operation, where two parent trees exchange subtrees to generate a new tree. The green box illustrates the mutation process, where a subtree of a given tree is replaced with a newly generated subtree. The lower part of the figure demonstrates the corresponding transformations in the tensor representation of trees for both crossover and mutation operations.

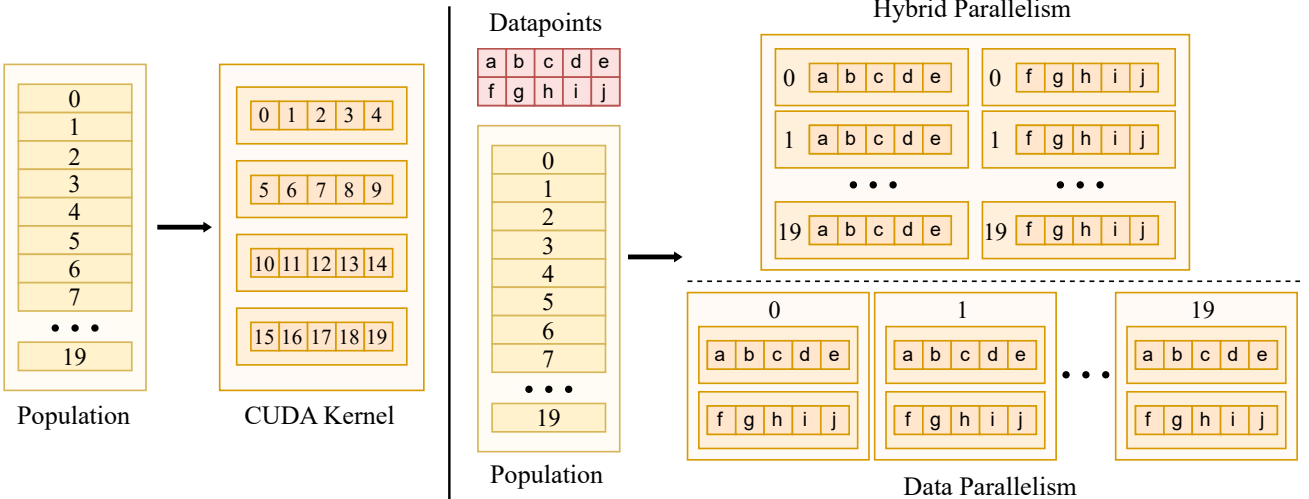


Fig. 4: Illustration of CUDA-based parallelism in EvoGP. The left part shows population parallelism for generation, crossover, mutation and inference kernel, where each individual is assigned to a separate thread. The right part depicts SR fitness evaluation, with hybrid parallelism (upper) computing all trees in one kernel launch, while data parallelism (lower) processes each tree separately across multiple launches.

Specifically, if the goal is to evaluate a population of size P on D data points, EvoGP configures a two-dimensional CUDA grid with dimensions $(P, \text{block_cnt})$. The parameters block_size and block_cnt are determined as follows:

$$\text{block_size} = \min(D, 1024),$$

$$\text{block_cnt} = \left\lceil \frac{D - 1}{\text{block_size}} \right\rceil + 1.$$

Here, 1024 is the maximum number of threads per block, chosen to balance computational efficiency and hardware constraints. Each block further divides the workload of evaluating a single tree across multiple data points, providing data-level parallelism within the block. Simultaneously, the different blocks in the grid are assigned to different trees, enabling population-level parallelism across blocks. This hybrid scheme efficiently utilizes GPU resources by processing multiple trees and multiple data points concurrently. The right half of Fig. 4 shows two different implementation methods for data parallelism and hybrid parallelism.

Although hybrid parallelism achieves better performance when the dataset is of moderate size, it may become less efficient than pure data-level parallelism when D is extremely large. In such cases, evaluating a single tree across a vast number of data points can fully occupy the GPU's computational resources, leaving no additional capacity to parallelize over the population dimension. Moreover, an exclusive data-level scheme can store tree representations in constant memory for each kernel invocation, yielding faster memory access compared to storing them in global memory under a hybrid strategy. Therefore, for very large datasets, relying solely on data-level parallelism can be more advantageous. The performance trade-off between these two approaches is further discussed and empirically validated in Section VI-C.

V. EvoGP IMPLEMENTATIONS

In this section, we introduce the overall architecture of EvoGP along with some additional features.

A. Overview of EvoGP

We present EvoGP, the first fully GPU-accelerated TGP framework. EvoGP is developed in Python and leverages the PyTorch [48] framework for efficient tensor management and GPU control. To further enhance computational performance, EvoGP integrates dedicated CUDA kernels for key evolutionary operations, including tree generation, mutation, crossover, inference, and symbolic regression (SR) fitness evaluation. Specifically, to accommodate input data of various scales in SR fitness evaluation, EvoGP implements both data parallelism and hybrid parallelism mentioned in Section IV-C. These CUDA kernels are provided as PyTorch custom operators, ensuring seamless interoperability with PyTorch's existing infrastructure. As a result, EvoGP benefits from both the flexibility of the Python AI ecosystem and the computational advantages of native GPU acceleration.

Beyond GPU acceleration of TGP algorithms, EvoGP also includes built-in support for common application domains where TGP has proven effective. These domains include symbolic regression, policy optimization, and classification tasks. Furthermore, EvoGP provides a collection of standardized problem benchmarks, including symbolic regression, classification, and policy optimization. It allows users to systematically evaluate different TGP strategies and tune their algorithms.

The overall architecture of EvoGP is illustrated in Fig. 5, providing a visual representation of its modular components and their interactions.

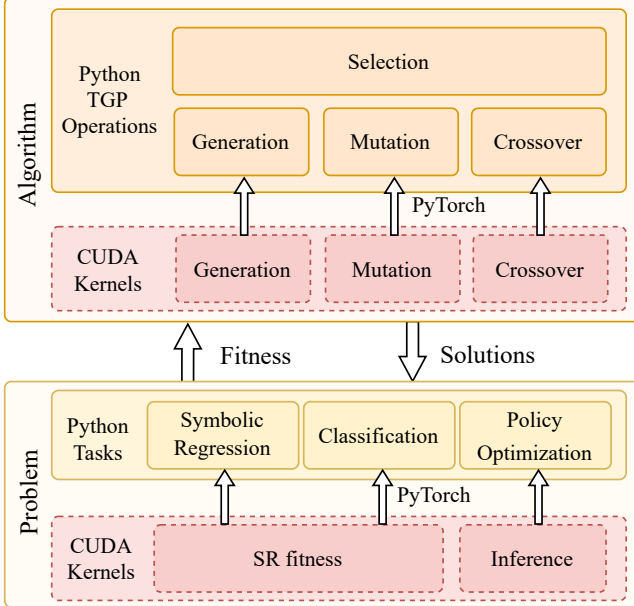


Fig. 5: Illustration of the EvoGP architecture. EvoGP consists of two main components: Algorithm and Problem. The Algorithm module implements the TGP algorithm along with multiple operation variants. The Problem module integrates various benchmark problems for user evaluation. Within these components, we design CUDA kernels to enable parallel acceleration of computational processes. These CUDA kernels are seamlessly integrated into Python using PyTorch’s custom operator functionality.

B. Rich Features and User Customization

EvoGP extends beyond basic GPU-accelerated TGP operations by offering a diverse set of evolutionary operator variants and a flexible interface for customization. In addition to the previously mentioned problem benchmarks, EvoGP provides multiple variations of key TGP operators, including selection, mutation, and crossover. These variants allow users to freely combine and configure different evolutionary strategies, enabling the design of customized TGP algorithms tailored to specific optimization tasks. Table I compares the range of operator variants implemented in mainstream TGP libraries, highlighting that EvoGP provides the most comprehensive set of supported operators.

To further enhance usability, EvoGP offers an intuitive interface for defining custom operators and problem formulations. Users can leverage low-level CUDA implementations to efficiently develop and execute their own optimized genetic operators, ensuring high performance while maintaining flexibility. Additionally, EvoGP's modular design allows researchers and practitioners to apply TGP algorithms to their own problem domains, making it a versatile tool for both academic research and real-world applications.

C. Multi-Output Support

EvoGP extends traditional TGP by incorporating multi-output functionality, allowing the application of TGP to tasks

that require multiple output values, such as policy optimization in reinforcement learning. This enhancement enables EvoGP to handle complex problem domains where a single-output GP framework would be insufficient.

To achieve multi-output computation, EvoGP uses Modi nodes [49] into the tree structure. These nodes possess two key characteristics:

- 1) Each Modi node specifies the output to which its value contributes. The contributions from multiple Modi nodes associated with the same output are aggregated according to a predefined rule, which in this case is summation, to produce the final output value.
- 2) If a Modi node has a parent node, it does not propagate its computed value upwards like regular nodes. Instead, it directly adopts the value of its rightmost child node. This mechanism effectively transforms the tree structure into a directed acyclic graph (DAG), enabling simultaneous computation of multiple outputs.

This distinction between regular nodes and Modi nodes is crucial when performing multi-output computations. While regular nodes operate under standard GP rules, Modi nodes follow a specialized processing scheme to ensure proper output assignment. This approach enables EvoGP to effectively support multi-output GP, making it well-suited for reinforcement learning and other tasks requiring multiple correlated outputs.

The computational process of Modi nodes is illustrated in Fig. 6, providing a visual representation of how multi-output values are generated within the EvoGP framework.

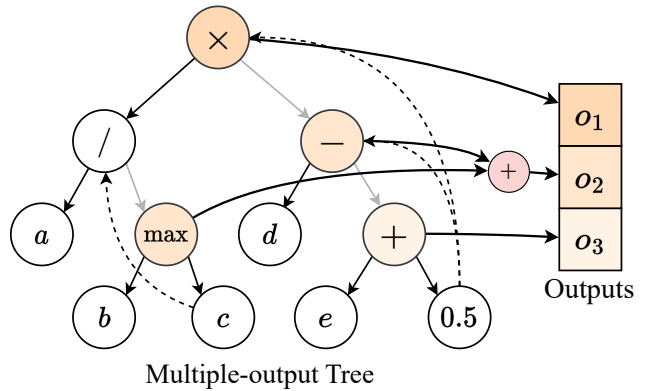


Fig. 6: An example of a multiple-output tree. The yellow nodes at different depths represent the Modi nodes. Each Modi node adds its value to the corresponding position in the output and propagates the value of its rightmost subtree to its parent node. The computed process in the figure are: $o_1 = a \div c \times 0.5$, $o_2 = \max(b, c) + (d - 0.5)$, $o_3 = e + 0.5$.

VI. EXPERIMENTS

This section presents a comprehensive evaluation of EvoGP, highlighting its performance across diverse tasks, datasets, and hardware configurations. The experiments are designed to validate the effectiveness of the proposed GPU-accelerated framework in addressing the computational challenges inherent in TGP. Specifically, we aim to answer four key questions:

TABLE I: Comparison of Mutation and Crossover Operators in Genetic Programming Tools

Name	One Point Cross.	One Point Leaf Biased Cross.	Subtree Mut.	Hoist Mut.	Single Point Mut.	Multi-Point Mut.	Insert Mut.	Delete Mut.	Single Const Mut.	Multi-Const Mut.
DEAP	✓	✓	✓	✗	✓	✗	✓	✓	✓	✓
Gplearn	✓	✗	✓	✓	✓	✗	✗	✗	✗	✗
KarooGP	✓	✗	✓	✗	✓	✗	✗	✗	✗	✗
TensorGP	✓	✗	✓	✗	✓	✗	✓	✓	✗	✗
SRGPU	✓	✗	✓	✓	✓	✓	✗	✗	✗	✗
EvoGP (Ours)	✓	✓	✓	✓	✓	✓	✓	✓	✓	✓

(1) How does EvoGP compare with existing TGP implementations in terms of execution time and solution quality? (2) What are the advantages of the hybrid parallelism strategy in EvoGP compared to existing data parallelism approaches? (3) How is the scalability of EvoGP in term of population size? (4) How does EvoGP perform across different application domains, including symbolic regression, classification, and robotics control? By systematically addressing these questions, we demonstrate EvoGP’s scalability, flexibility, and adaptability to diverse computational demands.

A. Experimental Setup

This section outlines the experimental setup used to evaluate EvoGP. The setup is designed to comprehensively assess the framework’s performance across a variety of tasks, hardware configurations, and parameter settings.

We assess the performance of EvoGP on three types of tasks to highlight its flexibility:

Symbolic Regression: This task uses the Pagee polynomial as a benchmark function, a widely adopted test case in genetic programming (GP) research due to its complexity and non-linear structure. The function is defined as:

$$f(x, y) = \frac{1}{1+x^{-4}} + \frac{1}{1+y^{-4}}.$$

The performance on this task is measured using the Mean Squared Error (MSE) loss between the predicted outputs and the true values of the function. A lower MSE indicates a better approximation of the target function.

Classification: Four datasets from the sklearn library [50] are used for classification tasks: *Iris*, *Wine*, *Breast Cancer*, and *Digits*. These datasets differ in terms of complexity, the number of features, and the number of classes, making them suitable for evaluating classification performance. The detailed information about these datasets is summarized in Table II. The performance metric for this task is classification accuracy, defined as the ratio of correctly predicted labels to the total number of test samples. Higher accuracy indicates better classification performance.

Robotics Control: Environments from the Brax framework [51] are used to test EvoGP in reinforcement learning tasks. The chosen environments include *Swimmer*, *Hopper*, *Walker2d*, and *HalfCheetah*, each presenting unique challenges in control dynamics. Table III provides the observation and action dimensions of these environments. Performance in these

TABLE II: Details of Classification Datasets

Dataset	Input Features	Output Classes	Data Count
Iris	4	3	150
Wine	13	3	178
Breast Cancer	30	2	569
Digits	64	10	1797

tasks is evaluated based on the cumulative reward obtained during an episode. The cumulative reward measures the total quality of the control policy, with higher rewards indicating better task performance.

TABLE III: Observation and Action Dimensions of Brax Environments

Environment	Observation Dimension	Action Dimension
Swimmer	8	2
Hopper	17	3
Walker2d	17	6
HalfCheetah	17	6

Details of the hardware specifications can be found in Table IV. We follow standard TGP settings commonly used in the literature. To evaluate the performance of the algorithms, we vary parameters such as population size and maximum generations, while other parameters remain fixed. The key fixed parameters used in our experiments are provided in Table V.

All experiments were repeated 10 times using different random seeds to ensure statistical robustness. Results are reported as mean values with 95% confidence intervals, providing a reliable basis for comparison.

This setup ensures that EvoGP is evaluated rigorously across diverse tasks and hardware configurations, highlighting its efficiency and adaptability to different computational demands.

TABLE IV: Hardware Specifications

Component	Specification
CPU	Intel(R) Xeon(R) Gold 6226R @ 2.90GHz
CPU Cores	8
GPU (SR Task)	NVIDIA RTX 3090
GPU (Other Tasks)	NVIDIA RTX 4090
Host RAM	512 GB
GPU RAM	24 GB
OS	Ubuntu 22.04.4 LTS

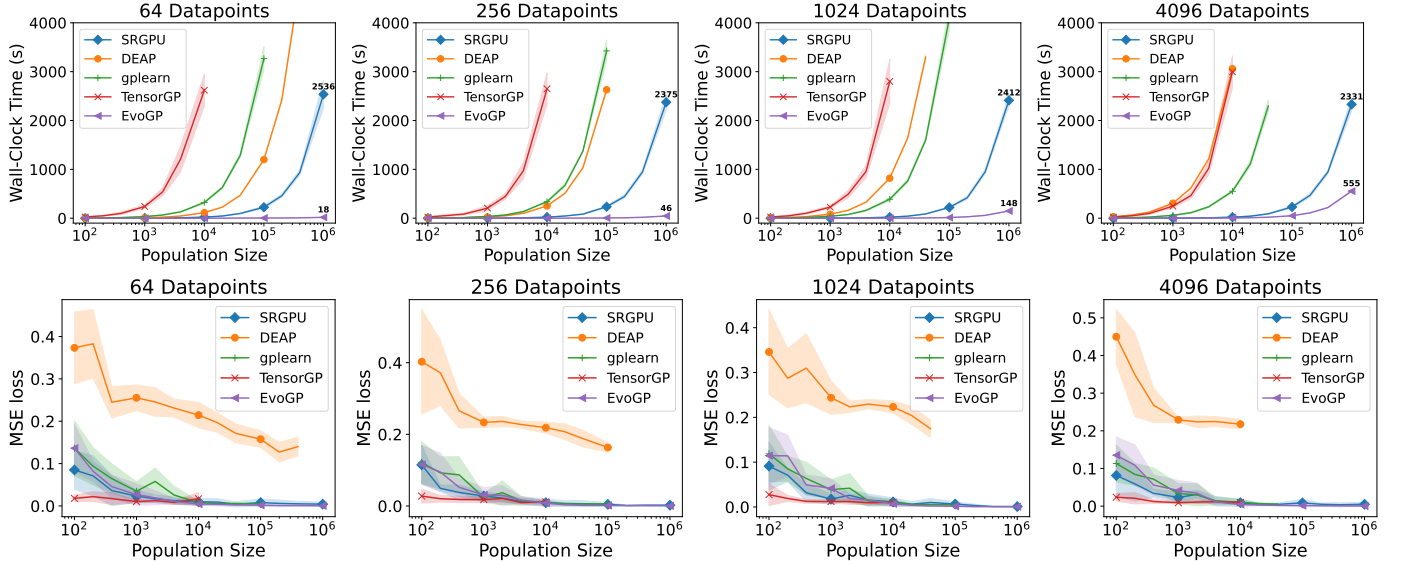


Fig. 7: Comparison with existing TGP implementations.

TABLE V: SR Experiment Parameters

Parameter	Value
Elite Rate	0.01
Survival Rate	0.3
Mutation Probability	0.2
Function Set (SR Task)	{+, -, ×, ÷, sin, cos, tan}
Function Set (Other Tasks)	{+, -, ×, ÷,}

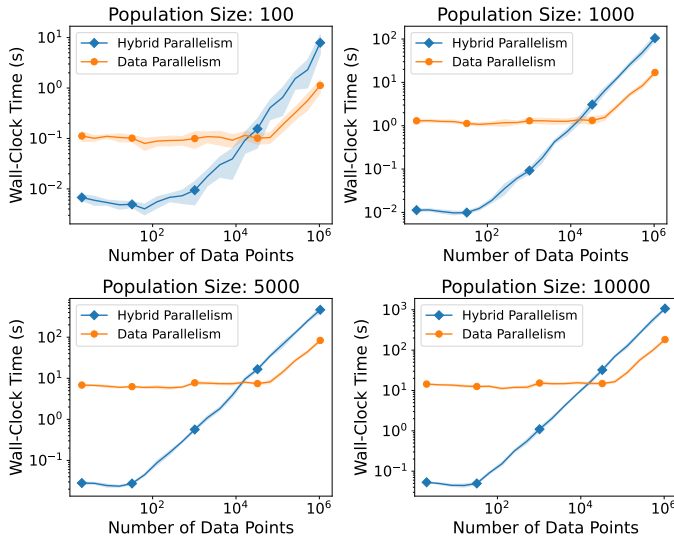


Fig. 8: Parallelism performance in terms of the number of data points.

B. Comparison with Existing TGP Implementations

We compare the performance of EvoGP with other mainstream TGP implementations including SRGPU [31], DEAP [29], gplearn [30] and TensorGP [28]. The primary focus of this experiment is to evaluate the execution time differences among these libraries when performing Symbolic Regression tasks. The experiments were conducted for 100 generations, and the number of data points (64, 256, 1024,

and 4096) was varied to control task complexity and computational workload. To prevent excessive runtime, any execution exceeding one hour is terminated early.

The experimental results are presented in Fig. 7. The top four plots illustrate the total execution time as a function of population size for different dataset scales, with the x-axis using a logarithmic scale. The results indicate that EvoGP consistently requires significantly less execution time than other libraries. For the baseline libraries, execution time scales linearly with population size (appearing exponential in the plots due to the logarithmic x-axis). In contrast, EvoGP exhibits a much slower increase in execution time as population size grows. Notably, when the population size is relatively small, EvoGP's execution time remains nearly constant.

The bottom four plots in Fig. 7 show how MSE loss varies with population size. The results demonstrate that EvoGP achieves comparable solution quality to other libraries, confirming that its acceleration does not compromise accuracy.

These findings highlight that EvoGP significantly reduces execution time while maintaining solution quality. This underscores the effectiveness of our GPU acceleration approach. Furthermore, when compared to another CUDA-accelerated implementation, EvoGP achieves remarkable speed improvements. Specifically, when the number of data points is at 64 and the population size is 10^6 , EvoGP reduces execution time by 140.89x compared to the fastest implementation [31]. This superior performance is attributed to EvoGP's optimized CUDA kernel design, which efficiently exploits population-level parallelism.

C. Effectiveness of Hybrid Parallelism

Hybrid parallelism in EvoGP was introduced to address the inefficiencies of traditional GPU-based approaches that rely solely on data-level parallelism. This experiment aims to evaluate the effectiveness of hybrid parallelism compared to data-level parallelism under various dataset sizes and population scales. The goal is to assess how well hybrid parallelism

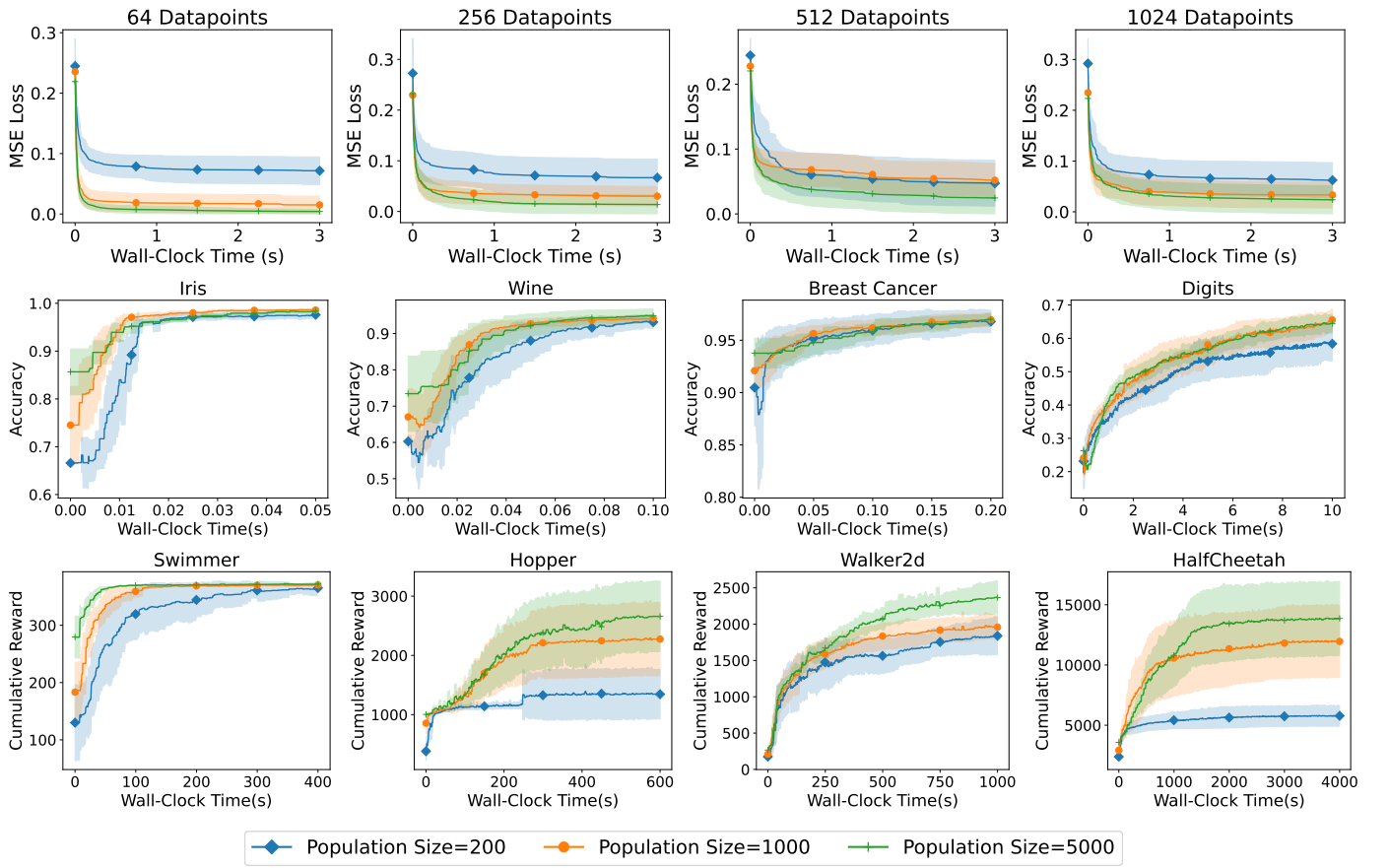


Fig. 9: Task performance versus wall-clock time for various population sizes. Rows correspond to symbolic regression, classification, and robotics control tasks, respectively.

adapts to different computational demands and identifies the conditions under which it outperforms data-level parallelism.

The experimental results are presented in Fig. 8. The x-axis represents the number of data points, while the y-axis denotes the wall clock time required for execution. We tested four population sizes: 100, 1,000, 5,000, and 10,000.

From the results, we observe a clear performance pattern. For small datasets, hybrid parallelism consistently outperforms data-level parallelism in execution time. This advantage is attributed to the ability of hybrid parallelism to process multiple trees concurrently across the GPU’s computational threads, maximizing resource utilization when the dataset size is insufficient to saturate the GPU using data-level parallelism alone.

However, as the dataset size increases, the efficiency gap between the two approaches narrows. For datasets exceeding a critical threshold (approximately $2^{14} = 16,384$ data points), data-level parallelism surpasses hybrid parallelism in performance. This transition is due to two key factors: 1. Large datasets allow data-level parallelism to fully utilize the GPU’s computational capacity by evaluating a single tree across all data points without requiring population-level parallelism. 2. Data-level parallelism stores tree structures in constant memory, enabling faster memory access compared to the global memory used in hybrid parallelism.

Despite these trade-offs, hybrid parallelism remains highly effective for moderate dataset sizes and provides flexibility in accommodating diverse computational scenarios. This adaptability underscores EvoGP’s innovative design, which leverages hybrid parallelism to balance workload distribution between data and population dimensions.

These findings highlight the importance of tailoring parallelism strategies to the specific characteristics of the task. While data-level parallelism is optimal for very large datasets, hybrid parallelism offers superior performance for small to medium-sized datasets, where GPU resources might otherwise be underutilized. By incorporating both strategies, EvoGP demonstrates its capability to optimize performance across a wide range of problem scales and configurations.

D. Performance across Tasks with Scalable Populations

This subsection evaluates EvoGP’s performance on symbolic regression, classification, and robotics control tasks with different population sizes. The experiments aimed to analyze the effect of population size on task performance and computation time. Population sizes of 200, 1000, and 5000 were tested for all tasks.

For symbolic regression, datasets with 64, 256, 512, and 1024 data points were used to simulate various task complexities. Classification tasks were performed on *Iris*, *Wine*,

TABLE VI: Performance and computational time across tasks and population sizes. Best performances are highlighted.

Task Type	Maximum Generations	Task Identifier	Pop Size	Performance	Wall-clock Time (S)
Symbolic Regression	100	64	200	0.100 \pm 0.023	0.123 \pm 0.011
			1000	0.023 \pm 0.016	0.240 \pm 0.008
			5000	0.009 \pm 0.006	0.435 \pm 0.018
		256	200	0.099 \pm 0.039	0.146 \pm 0.007
			1000	0.041 \pm 0.022	0.319 \pm 0.015
			5000	0.021 \pm 0.019	0.879 \pm 0.036
		512	200	0.111 \pm 0.054	0.150 \pm 0.020
			1000	0.070 \pm 0.025	0.439 \pm 0.026
			5000	0.034 \pm 0.025	1.384 \pm 0.079
		1024	200	0.102 \pm 0.048	0.184 \pm 0.037
			1000	0.042 \pm 0.026	0.609 \pm 0.051
			5000	0.025 \pm 0.027	2.207 \pm 0.168
Classification	40	Iris	200	0.979 \pm 0.005	0.059 \pm 0.008
			1000	0.990 \pm 0.003	0.123 \pm 0.009
			5000	0.993 \pm 0.000	0.356 \pm 0.008
		Wine	200	0.915 \pm 0.019	0.060 \pm 0.011
			1000	0.946 \pm 0.006	0.125 \pm 0.014
			5000	0.974 \pm 0.005	0.354 \pm 0.020
		Breast Cancer	200	0.955 \pm 0.009	0.075 \pm 0.007
			1000	0.968 \pm 0.006	0.205 \pm 0.018
			5000	0.982 \pm 0.002	0.881 \pm 0.079
		Digits	200	0.287 \pm 0.017	3.127 \pm 0.091
			1000	0.679 \pm 0.027	12.005 \pm 1.718
			5000	0.811 \pm 0.024	57.514 \pm 1.227
Robotics Control	100	Swimmer	200	369.509 \pm 1.414	791.546 \pm 99.421
			1000	373.577 \pm 2.363	891.185 \pm 65.661
			5000	376.662 \pm 2.585	735.877 \pm 57.907
		Hopper	200	1399.618 \pm 448.981	354.702 \pm 25.832
			1000	2444.291 \pm 464.516	386.617 \pm 21.714
			5000	2748.185 \pm 505.279	503.509 \pm 2.800
		Walker2d	200	1550.955 \pm 334.275	324.897 \pm 62.063
			1000	1905.647 \pm 189.443	553.908 \pm 19.456
			5000	2550.197 \pm 385.302	1233.198 \pm 9.948
		Halfcheetah	200	5545.219 \pm 716.671	1175.703 \pm 77.945
			1000	11313.934 \pm 3181.319	1458.846 \pm 7.558
			5000	14114.018 \pm 3136.102	3701.693 \pm 22.334

* Performance metrics (see Section VI-A): (1) Symbolic Regression: MSE Loss (lower is better); (2) Classification: Accuracy (higher is better); (3) Robotics Control: Cumulative Reward (higher is better).

Breast Cancer, and *Digits* datasets, while robotics control tasks utilized Brax environments such as *Swimmer*, *Hopper*, *Walker2d*, and *HalfCheetah*. The experimental results are summarized in Table VI, and performance trends over time are shown in Fig. 9.

The results are summarized in Table VI, which presents the performance achieved and the computation time required for different population sizes and tasks. Fig. 9 provides a graphical representation of the relationship between wall-clock time and task performance under various experimental settings. The horizontal axis represents wall-clock time, while the vertical axis indicates task-specific performance metrics, including MSE for symbolic regression, classification accuracy for classification tasks, and cumulative reward for robotics control tasks.

EvoGP demonstrated remarkable computational efficiency, achieving rapid convergence for symbolic regression tasks with larger population sizes. For instance, with a population

size of 5000, the MSE loss for tasks involving 64 data points converged within 3 seconds. Similarly, in classification tasks, EvoGP achieved over 97% accuracy for *Iris*, *Wine*, and *Breast Cancer* datasets in under 1 second and 81.1% accuracy for the more complex *Digits* dataset within 1 minute. For robotics control tasks, EvoGP consistently delivered strong performance across all tested environments.

Larger population sizes consistently outperformed smaller ones across all tasks. In symbolic regression tasks, larger populations achieved lower MSE losses, indicating better convergence. In classification tasks, they yielded higher accuracy, and in robotics control tasks, they achieved superior cumulative rewards. These findings emphasize the importance of larger population sizes for effectively exploring the solution space and enhancing task performance.

The results also highlight the effectiveness of EvoGP’s GPU-accelerated population parallelism. Despite exponential increases in population size, computation time did not grow

proportionally. In symbolic regression and robotics control tasks, larger populations often achieved higher performance in shorter wall-clock times. This efficiency is attributed to EvoGP's GPU-based population parallelism, which significantly reduces execution time compared to traditional sequential approaches.

These experimental findings underscore EvoGP's ability to handle large-scale populations effectively, offering a powerful tool for real-world applications that require high-performance TGP.

VII. CONCLUSION

In this paper, we introduced EvoGP, a GPU-accelerated framework for Tree-based Genetic Programming (TGP). It tackles three major challenges in GPU acceleration for TGP: inefficient tree encoding, heterogeneous genetic operations, and limited parallelism in fitness evaluation. Our tensor-based encoding allows all trees to share a uniform shape, which avoids repeated memory allocations and reduces irregular memory access. We also developed a unified parallel framework for genetic operations, along with a fully parallel fitness evaluation strategy for symbolic regression. Experimental results show that EvoGP achieves speedups of up to 140.89 times compared with existing GPU-based TGP implementations, demonstrating its effectiveness in high-performance evolutionary computation.

Building upon these results, our objective is to extend EvoGP to address more complex and diverse tasks. The computational efficiency and population-level parallelism achieved by EvoGP open up opportunities to leverage larger populations, enabling greater solution diversity and improved accuracy in challenging scenarios such as robotic control and autonomous systems. Furthermore, while the current implementation of multi-output support has proven effective, exploring novel strategies to further enhance this capability remains an exciting direction for future research. We anticipate that this framework will provide researchers with robust tools and methodologies conducive to the advancement of interpretable artificial intelligence.

REFERENCES

- [1] J. R. Koza, "Genetic programming as a means for programming computers by natural selection," *Statistics and Computing*, vol. 4, pp. 87–112, 1994.
- [2] Y. Mei, Q. Chen, A. Lensen, B. Xue, and M. Zhang, "Explainable artificial intelligence by genetic programming: A survey," *IEEE Transactions on Evolutionary Computation*, vol. 27, no. 3, pp. 621–641, 2022.
- [3] W. Banzhaf, F. D. Francone, R. E. Keller, and P. Nordin, *Genetic programming: an introduction: on the automatic evolution of computer programs and its applications*. Morgan Kaufmann Publishers Inc., 1998.
- [4] M. F. Brameier and W. Banzhaf, *Basic concepts of linear genetic programming*. Springer, 2007.
- [5] J. F. Miller *et al.*, "An empirical study of the efficiency of learning boolean functions using a cartesian genetic programming approach," in *Proceedings of the Genetic and Evolutionary Computation Conference*, vol. 2, 1999, pp. 1135–1142.
- [6] J. Miller and A. Turner, "Cartesian genetic programming," in *Proceedings of the Companion Publication of the 2015 Annual Conference on Genetic and Evolutionary Computation*, 2015, pp. 179–198.
- [7] C. Ferreira, "Gene expression programming: A new adaptive algorithm for solving problems," *Complex Systems*, vol. 13, no. 2, pp. 87–129, 2001.
- [8] M. O'Neill and C. Ryan, "Grammatical evolution," *IEEE Transactions on Evolutionary Computation*, vol. 5, no. 4, pp. 349–358, 2001.
- [9] D. Ari and B. B. Alagöz, "A review of genetic programming: Popular techniques, fundamental aspects, software tools and applications," *Sakarya University Journal of Science*, vol. 25, no. 2, pp. 397–416, 2021.
- [10] D. R. White, J. McDermott, M. Castelli, L. Manzoni, B. W. Goldman, G. Kronberger, W. Jaśkowski, U.-M. O'Reilly, and S. Luke, "Better GP benchmarks: community survey results and proposals," *Genetic Programming and Evolvable Machines*, vol. 14, pp. 3–29, 2013.
- [11] M. Schmidt and H. Lipson, "Distilling free-form natural laws from experimental data," *Science*, vol. 324, no. 5923, pp. 81–85, 2009.
- [12] Q. Chen, M. Zhang, and B. Xue, "Feature selection to improve generalization of genetic programming for high-dimensional symbolic regression," *IEEE Transactions on Evolutionary Computation*, vol. 21, no. 5, pp. 792–806, 2017.
- [13] W. La Cava, B. Burlacu, M. Virgolin, M. Kommenda, P. Orzechowski, F. O. de França, Y. Jin, and J. H. Moore, "Contemporary symbolic regression methods and their relative performance," *Advances in Neural Information Processing Systems*, vol. 2021, no. DB1, p. 1, 2021.
- [14] N. Makke and S. Chawla, "Interpretable scientific discovery with symbolic regression: a review," *Artificial Intelligence Review*, vol. 57, no. 1, p. 2, 2024.
- [15] B. Tran, B. Xue, and M. Zhang, "Genetic programming for feature construction and selection in classification on high-dimensional data," *Memetic Computing*, vol. 8, pp. 3–15, 2016.
- [16] P. G. Espejo, S. Ventura, and F. Herrera, "A survey on the application of genetic programming to classification," *IEEE Transactions on Systems, Man, and Cybernetics, Part C (Applications and Reviews)*, vol. 40, no. 2, pp. 121–144, 2009.
- [17] Y. Bi, B. Xue, and M. Zhang, *Genetic programming for image classification: An automated approach to feature learning*. Springer Nature, 2021, vol. 24.
- [18] H. Al-Sahaf, Y. Bi, Q. Chen, A. Lensen, Y. Mei, Y. Sun, B. Tran, B. Xue, and M. Zhang, "A survey on evolutionary machine learning," *Journal of the Royal Society of New Zealand*, vol. 49, no. 2, pp. 205–228, 2019.
- [19] A. Khan, A. S. Qureshi, N. Wahab, M. Hussain, and M. Y. Hamza, "A recent survey on the applications of genetic programming in image processing," *Computational Intelligence*, vol. 37, no. 4, pp. 1745–1778, 2021.
- [20] S. Nguyen, Y. Mei, and M. Zhang, "Genetic programming for production scheduling: a survey with a unified framework," *Complex & Intelligent Systems*, vol. 3, pp. 41–66, 2017.
- [21] Y. Tang, Y. Tian, and D. Ha, "EvoJAX: Hardware-accelerated neuroevolution," in *Proceedings of the Genetic and Evolutionary Computation Conference Companion*, 2022, pp. 308–311.
- [22] R. T. Lange, "evosax: JAX-based evolution strategies," in *Proceedings of the Companion Conference on Genetic and Evolutionary Computation*, 2023, pp. 659–662.
- [23] B. Huang, R. Cheng, Z. Li, Y. Jin, and K. C. Tan, "EvoX: A distributed GPU-accelerated framework for scalable evolutionary computation," *IEEE Transactions on Evolutionary Computation*, 2024.
- [24] N. E. Toklu, T. Atkinson, V. Micka, P. Liskowski, and R. K. Srivastava, "EvoTorch: Scalable evolutionary computation in Python," *arXiv:2302.12600*, 2023.
- [25] L. Wang, M. Zhao, E. Liu, K. Sun, and R. Cheng, "Tensorized neuroevolution of augmenting topologies for GPU acceleration," in *Proceedings of the Genetic and Evolutionary Computation Conference*, ser. GECCO '24, 2024, p. 1156–1164.
- [26] Z. Liang, T. Jiang, K. Sun, and R. Cheng, "GPU-accelerated evolutionary multiobjective optimization using tensorized RVEA," in *Proceedings of the Genetic and Evolutionary Computation Conference*, 2024, pp. 566–575.
- [27] K. Staats, E. Pantridge, M. Cavaglia, I. Milovanov, and A. Aniyan, "TensorFlow enabled genetic programming," in *Proceedings of the Genetic and Evolutionary Computation Conference Companion*, 2017, pp. 1872–1879.
- [28] F. Baeta, J. Correia, T. Martins, and P. Machado, "TensorGP – genetic programming engine in TensorFlow," in *Applications of Evolutionary Computation*, P. A. Castillo and J. L. Jiménez Laredo, Eds. Springer International Publishing, 2021, pp. 763–778.
- [29] F.-A. Fortin, F.-M. De Rainville, M.-A. G. Gardner, M. Parizeau, and C. Gagné, "DEAP: Evolutionary algorithms made easy," *The Journal of Machine Learning Research*, vol. 13, no. 1, pp. 2171–2175, 2012.
- [30] T. Stephens, "gplearn: Genetic programming in Python, with a scikit-learn inspired API," <https://github.com/trevorstephens/gplearn>, 2015.

- [31] R. Zhang, A. Lensen, and Y. Sun, “Speeding up genetic programming based symbolic regression using GPUs,” in *Pacific Rim International Conference on Artificial Intelligence*. Springer, 2022, pp. 519–533.
- [32] D. Guide, “CUDA C++ programming guide,” NVIDIA, July, 2020.
- [33] G. S. Hornby, H. Lipson, and J. B. Pollack, “Generative representations for the automated design of modular physical robots,” *IEEE Transactions on Robotics and Automation*, vol. 19, no. 4, pp. 703–719, 2003.
- [34] J. R. Koza, M. A. Keane, M. J. Streeter, W. Mydlowec, J. Yu, and G. Lanza, *Genetic programming IV: Routine human-competitive machine intelligence*. Springer Science & Business Media, 2005, vol. 5.
- [35] J. D. Lohn, G. S. Hornby, and D. S. Linden, “Human-competitive evolved antennas,” *AI EDAM*, vol. 22, no. 3, pp. 235–247, 2008.
- [36] J. R. Koza, “Human-competitive results produced by genetic programming,” *Genetic Programming and Evolvable Machines*, vol. 11, pp. 251–284, 2010.
- [37] S. Perkins and G. Hayes, “Evolving complex visual behaviours using genetic programming and shaping,” in *Interdisciplinary Approaches to Robot Learning*. World Scientific, 2000, pp. 162–184.
- [38] D. C. Dracopoulos, D. Effraimidis, and B. D. Nichols, “Genetic programming as a solver to challenging reinforcement learning problems,” *International Journal of Computer Research*, vol. 20, no. 3, p. 351, 2013.
- [39] D. Hein, S. Udluft, and T. A. Runkler, “Interpretable policies for reinforcement learning by genetic programming,” *Engineering Applications of Artificial Intelligence*, vol. 76, pp. 158–169, 2018.
- [40] R. Poli, W. B. Langdon, and N. F. McPhee, *A Field Guide to Genetic Programming*. Lulu Enterprises, UK Ltd, 2008.
- [41] M. Pharr and R. Fernando, *GPU Gems 2: Programming techniques for high-performance graphics and general-purpose computation (gpu gems)*. Addison-Wesley Professional, 2005.
- [42] M. Winter, M. Parger, D. Mlakar, and M. Steinberger, “Are dynamic memory managers on GPUs slow? a survey and benchmarks,” in *Proceedings of the 26th ACM SIGPLAN Symposium on Principles and Practice of Parallel Programming*, 2021, pp. 219–233.
- [43] J. Nickolls, I. Buck, M. Garland, and K. Skadron, “Scalable parallel programming with CUDA,” in *ACM SIGGRAPH 2008 Classes*, ser. SIGGRAPH ’08. Association for Computing Machinery, 2008.
- [44] J. Sanders, *CUDA by Example: An Introduction to General-Purpose GPU Programming*. Addison-Wesley Professional, 2010.
- [45] E. Lindholm, J. Nickolls, S. Oberman, and J. Montrym, “NVIDIA Tesla: A unified graphics and computing architecture,” *IEEE Micro*, vol. 28, no. 2, pp. 39–55, 2008.
- [46] M. Garland, S. Le Grand, J. Nickolls, J. Anderson, J. Hardwick, S. Morton, E. Phillips, Y. Zhang, and V. Volkov, “Parallel computing experiences with CUDA,” *IEEE Micro*, vol. 28, no. 4, pp. 13–27, 2008.
- [47] M. Abadi, A. Agarwal, P. Barham, E. Brevdo, Z. Chen, C. Citro, G. S. Corrado, A. Davis, J. Dean, M. Devin *et al.*, “TensorFlow: Large-scale machine learning on heterogeneous distributed systems,” *arXiv:1603.04467*, 2016.
- [48] A. Paszke, S. Gross, S. Chintala, G. Chanan, E. Yang, Z. DeVito, Z. Lin, A. Desmaison, L. Antiga, and A. Lerer, “Automatic differentiation in PyTorch,” in *NIPS-W*, 2017.
- [49] Y. Zhang and M. Zhang, “A multiple-output program tree structure in genetic programming,” in *Proceedings of The Second Asian-Pacific Workshop on Genetic Programming*. Citeseer, 2004.
- [50] F. Pedregosa, G. Varoquaux, A. Gramfort, V. Michel, B. Thirion, O. Grisel, M. Blondel, P. Prettenhofer, R. Weiss, V. Dubourg, J. Vanderplas, A. Passos, D. Cournapeau, M. Brucher, M. Perrot, and E. Duchesnay, “Scikit-learn: Machine learning in Python,” *Journal of Machine Learning Research*, vol. 12, pp. 2825–2830, 2011.
- [51] C. D. Freeman, E. Frey, A. Raichuk, S. Girgin, I. Mordatch, and O. Bachem, “Brax—a differentiable physics engine for large scale rigid body simulation,” *arXiv:2106.13281*, 2021.